ISSN 2070-0482, Mathematical Models and Computer Simulations, 2023, Vol. 15, No. 4, pp. 746–758. © Pleiades Publishing, Ltd., 2023.
Russian Text © The Author(s), 2023, published in Matematicheskoe Modelirovanie, 2023, Vol. 35, No. 2, pp. 75–94.

Calculation of the Initial Elevation of the Water Surface at the Source of a Tsunami in a Basin with Arbitrary Bottom Topography

K. A. Semenstov[a,*] and M. A. Nosov[a,b]

[a] *Lomonosov Moscow State University, Moscow, Russia*

[b] *Institute of Marine Geology and Geophysics, Far East Branch, Russian Academy of Sciences, Yuzhno-Sakhalinsk, Russia*

**e-mail: sebbest@yandex.ru*

Received September 7, 2022; revised November 8, 2022; accepted November 14, 2022

Abstract—A two-dimensional (0*xz*) numerical model that makes it possible to calculate the initial elevation of the water surface in the source of a tsunami in a basin of variable depth is developed in the potential theory of an incompressible fluid under the approximation of an instantaneous deformation of the sea bottom. The model makes it possible to take into account the contribution of the horizontal component of the bottom deformation and the smoothing effect of the water layer through the use of the σ coordinate. To test the numerical model, we obtained an analytical solution to the problem of the initial elevation in a basin with a flat sloping bottom with a bottom deformation of a triangular shape. The results of the test show that for a spatial step typical for numerical tsunami models, there is close agreement between the numerical and analytical solutions. Using the developed σ model, we calculate the initial elevations of the water surface during the Kuril earthquake on January 13, 2007 and the Great East Japan Tohoku earthquake on March 11, 2011 (along the selected 2D sections). The results obtained are used to test an approximate method for calculating the initial elevation, known as the Kajiura filter, in which the ocean depth is assumed to be constant throughout the area of the source of the tsunami.

Keywords: tsunami, initial elevation, potential theory, incompressible fluid, Kajiura filter, sigma coordinate

DOI: 10.1134/S2070048223040166

1. INTRODUCTION

In the numerical simulation of a tsunami of seismic origin, the process of wave excitation is usually considered to be instantaneous, see, for example, [1–3]. Only a few models take into account the dynamics of the bottom deformation [4–6].

In the "instantaneous deformation of the bottom" approximation, it is understood that the deviation of the free water surface from the equilibrium position (initial elevation) and the zero field of flow velocities must be set as the initial conditions for modeling. In this case, the initial elevation is equated to the vertical component of the bottom deformation (e.g., [7]) or, more correctly, to the vertical displacement of the bottom surface, calculated taking into account the relief inhomogeneities [8–12]. This approach quite adequately reproduces the main mechanism of the generation of a tsunami—water displacement by coseismic deformation of the bottom—but it does not take into account the smoothing effect of the water layer [13–15]. Due to this effect, the initial elevation of the water surface is always characterized by a smaller amplitude and is smoother (smoothed) compared to the bottom displacement [16, 17].

Until the end of the 20th century, the source of an earthquake was mainly represented as a rectangular rupture area with a uniform displacement distribution (centroid moment tensor solution [18]). Such a simplified representation made it possible to calculate the bottom deformation vector field only approximately; therefore, taking into account a rather weak smoothing effect could not noticeably improve the quality of tsunami modeling. In recent decades, there has been a fundamental breakthrough in the reconstruction of the slip structure in the earthquake source (finite fault model [19–21]). Despite the fact that the data on the slip structure are available in the public domain with a significant delay (from two hours to several weeks, https://earthquake.usgs.gov/), some scientific groups offer algorithms that allow us to

restore the finite fault model in real time [20, 21]. Thus, using the example of the Tohoku catastrophic event on March 11, 2011, it was shown in [21] that, in the presence of a dense network of GPS stations, the source of an earthquake and, accordingly, the deformation of the earth's crust can be reconstructed with an accuracy of >99% in 2–3 minutes.

In addition, in the last ten years, there has been significant progress in the field of numerical modeling of tsunami propagation. For example, it became possible to take into account the effect of density stratification, water compressibility, the deflection of the ocean floor directly under a wave, and the related change in the gravitational potential on the tsunami wave propagation velocity [22, 23]. The combined consideration of these factors made it possible to reproduce the propagation time of the Tohoku tsunami on March 11, 2011 over transoceanic distances with an error of 1 minute [23]. Obviously, it makes sense to use such refined tsunami propagation models only if the generation models are of the appropriate quality. In relation to this, the calculation of the initial elevation of the water surface in the source of the tsunami with the maximum accuracy, which is only possible with the available seismic information, has become an urgent need.

At the moment, the most common way to calculate the initial elevation, taking into account the smoothing effect, is an approximate method, known as the Kajiura filter, in which the ocean depth is assumed to be constant throughout the source area of the tsunami. This method is based on the analytical solution of the problem of tsunami generation by the instantaneous deformation of a flat horizontal bottom, obtained in the framework of the linear potential theory of an incompressible fluid [13, 14, 24–27]

$$\xi(x,y) = \frac{1}{2\pi}\int_{-\infty}^{+\infty}\int_{-\infty}^{+\infty} dk_x dk_y \frac{\hat{\eta}(k_x,k_y)}{\mathrm{ch}(kH_0)} e^{i(k_x x + k_y y)}, \tag{1}$$

where $\xi(x,y)$ is the initial elevation of the water surface, H_0 is depth of the ocean, $\hat{\eta}(k_x,k_y) = \frac{1}{2\pi}\int_{-\infty}^{+\infty}\int_{-\infty}^{+\infty} dxdy\eta(x,y)e^{-i(k_x x + k_y y)}$ is the spatial Fourier transform of the vertical displacement of the bottom $\eta(x,y)$, and $k^2 = k_x^2 + k_y^2$. Formula (1) is known as the Kajiura equation [14, 28] and its application for spatial bottom displacement filtering is called the Kajiura filter [29, 30]. Formula (1) was obtained for an ocean of constant depth H_0; therefore, when applying it in calculating the initial elevations in real tsunami sources, the average source depth is used. Taking into account the fact that in the region of a real tsunami source, the ocean depth can vary significantly, sometimes by an order of magnitude, the validity of using the average source depth is doubtful and needs, at the very least, careful verification [16, 27]. The relevance of such a check is also confirmed by the fact that the Kajiura filter is used not only in models developed in the instantaneous bottom deformation approximation but also in quasi-dynamic models—two-dimensional codes ($0xy$)—which allow introducing a dynamic correction to the displacement of the water surface in each time layer [30–32].

The main aim of this study is to develop a technique for numerically solving the problem of calculating the initial elevation of the water surface in an ocean of variable depth, caused by the instantaneous deformation of the bottom of an arbitrary shape. The technique is developed on a simplified two-dimensional model ($0xz$). The second aim of this study is to obtain an analytical solution to the problem of calculating the initial elevation in a basin with a flat sloping bottom caused by the bottom deformation of a triangular shape. This analytical solution is necessary for testing the numerical model. This paper also demonstrates the application of the constructed numerical model to the calculation of the initial elevation in the sources of real tsunamis: the Kuril earthquake on January 13, 2007 and the Great East Japan Tohoku earthquake on March 11, 2011. The results obtained are used to test the Kajiura filter, an approximate method for calculating the initial elevation.

2. NUMERICAL SOLUTION

Certain approaches to the calculation of the smoothed initial elevation of the water surface were used in numerical modeling and analyzed theoretically by various scientific groups [13, 14, 24–26, 33–37]. K. Kajiura used Green's function for the velocity potential and presented the solution as a series consisting of the sum of the integrals corresponding to multiple reflections of the source from the surface and from the bottom [14]. T. Saito calculated the response of the water layer to a point source given by the Dirac delta function, and then applied the superposition principle [34, 37]. The Laplace [24, 26] and Fourier [13, 25] transformations were also used to solve this problem. We note the original approach proposed in [33]. The authors of this paper calculated the initial elevation of the water surface in a basin with a slowly

varying depth using an electrostatic analogy and presented the resulting solution as an iterative procedure. This approach has found practical application in modeling real events [35, 36].

We have developed the concept proposed in [15, 16, 38]. In this concept, the dynamic problem of calculating the response of the water layer to the seismic movements of the bottom, formulated in terms of the velocity potential Φ [13, 14, 24–27], can be reduced to a simpler static problem. To do this, it is necessary to introduce the displacement potential $F = \int_0^\tau \Phi dt$ and require compliance with the instantaneous condition of bottom deformation $\tau \ll \sqrt{H/g}$, where τ is the duration of the bottom deformation at a particular point, H is the depth of the ocean, and g is the free fall acceleration [17]. We locate the origin of the Cartesian coordinate system $0xz$ on the undisturbed water surface with axis $0z$ directed vertically upwards. In such a coordinate system, the static problem of finding the initial elevation will be formulated as follows [15, 38]:

$$\frac{\partial^2 F}{\partial x^2} + \frac{\partial^2 F}{\partial z^2} = 0, \tag{2}$$

$$F\big|_{z=0} = 0, \tag{3}$$

$$\left.\frac{\partial F}{\partial \mathbf{n}}\right|_{z=-H(x)} = d_n(x), \tag{4}$$

where $F(x,z)$ is the displacement potential, $H(x)$ is the depth of the ocean, $d_n(x) = (\mathbf{d},\mathbf{n})$ is the displacement of the bottom in the direction of the normal, $\mathbf{d}(x) = \{d_x, d_z\}$ is the vector residual deformation of the bottom, $\mathbf{n}(x) = \{n_x, n_z\}$ is the unit vector of the normal to the bottom surface, and $\frac{\partial F}{\partial \mathbf{n}} = \frac{\partial F}{\partial x} n_x + \frac{\partial F}{\partial z} n_z$ is the displacement of water in the bottom layer in the direction of the normal. The initial elevation of the water surface is expressed in terms of the displacement potential using a simple formula

$$\xi(x) = \partial F/\partial z\big|_{z=0}. \tag{5}$$

For the numerical solution of problem (2)–(5) in a reservoir, the depth of which is given by an arbitrary function $H(x)$, we pass to a curvilinear nonorthogonal coordinate system $(\hat{x},\sigma)$: $\hat{x} = x$, $\sigma = z/H(x)$. Value σ varies from 0 on the undisturbed free water surface to -1 at the bottom. The $(\hat{x},\sigma)$ coordinate system makes it possible to map the computational domain of an arbitrary shape onto a rectangular domain [39, 40], which greatly simplifies the setting of the boundary condition for impermeability at the bottom in an ocean of variable depth. For the first time σ coordinate was proposed in [39] and is widely used to this day in various versions in numerical models of the dynamics of the atmosphere and ocean [41–45]. The version we use is called depth-normalized σ-coordinates [46, 47].

Problem (2)–(5) in coordinates $(\hat{x},\sigma)$ takes the form [48]

$$\frac{\partial^2 F}{\partial \hat{x}^2} + \frac{1+(\sigma H')^2}{H^2}\frac{\partial^2 F}{\partial \sigma^2} - \frac{2\sigma H'}{H}\frac{\partial^2 F}{\partial \hat{x}\partial\sigma} + \sigma\frac{2(H')^2 - H''H}{H^2}\frac{\partial F}{\partial \sigma} = 0, \tag{6}$$

$$F\big|_{\sigma=0} = 0, \tag{7}$$

$$\frac{\partial F}{\partial \hat{x}} n_x + \frac{n_z + H' n_x}{H}\left.\frac{\partial F}{\partial \sigma}\right|_{\sigma=-1} = d_n(\hat{x}), \tag{8}$$

$$\xi(\hat{x}) = \frac{1}{H(\hat{x})}\left.\frac{\partial F}{\partial \sigma}\right|_{\sigma=0}, \tag{9}$$

where H' and H'' are the first and second derivatives of $H(\hat{x})$ in $\hat{x}$. We note that the scalar product $(\mathbf{d},\mathbf{n})$ does not depend on the choice of the coordinate system. Due to this, the vector components normal to the bottom $\{n_x, n_z\}$ and bottom deformation $\{d_x, d_z\}$ required for the calculation of $(\mathbf{d},\mathbf{n})$ can be specified in the $0xz$ Cartesian coordinate system, which significantly simplifies the practical implementation of the calculations.

Problem (6)–(9) will be solved numerically by the one-step iteration method [49]. The iteration method is stable, as well as easy to implement and debug. As mentioned above, detailed information about the structure of slips in the earthquake source (finite fault model) appears in the public domain with a delay of two hours to several weeks (https://earthquake.usgs.gov/). In relation to this, at this stage, an

increased rate of convergence of the numerical method is not required. Let us write the difference approximations of the derivatives on the "cross" template. We choose the outer boundary of the computational domain Γ passing through the ocean at such a distance from the zone of the maximum deformation of the bottom that the displacement of the free surface and the deformation of the bottom on it can be neglected. This will allow us to set the simplest Dirichlet condition $F|_\Gamma = 0$ on the outer boundary.

The condition for terminating the iterative process is formulated as follows. Assume F^i is the total value of the displacement potential over all nodes at the ith step of the iterative process. At each step, we will calculate the value $(F^i - F^{i-1})/F^{i-1}$. When this value becomes less than 10^{-7}, we assume that the required accuracy is achieved and the iterative process can be stopped.

We set $F_0(\hat{x},\sigma) = d_z(\hat{x})H(\hat{x})\sigma$ as the zero approximation. From a physical point of view, this means that, in the zeroth approximation, the initial elevation of the water surface is equal to the vertical component of the bottom deformation (formula (9)). It is also obvious that condition (3) is automatically satisfied in this case.

3. ANALYTICAL SOLUTION FOR NUMERICAL MODEL TESTING

One of the possible ways to check the constructed numerical σ model is by comparing it with the known analytical solution of problem (2)–(5) obtained for any particular type of function $H(x)$.

The simplest case for which there is an analytical solution to problem (2)–(5) is a reservoir of constant depth H_0. The analytical solution of problem (2)–(5) in this case has the form

$$\xi(x) = \frac{1}{\sqrt{2\pi}}\int_{-\infty}^{+\infty} dk\,\frac{\hat{\eta}(k)}{\mathrm{ch}(kH_0)}e^{ikx}, \tag{10}$$

where $\hat{\eta}(k) = \frac{1}{\sqrt{2\pi}}\int_{-\infty}^{+\infty} dx\eta(x)e^{-ikx}$ is the Fourier transform of the vertical displacement of the bottom. However, this solution is unsuitable for testing σ models, since at $H(x) \equiv H_0$ all terms in Eq. (6) containing H' and H'' vanish, as a result of which Eq. (6) itself is significantly simplified and reduced to the ordinary Laplace equation written in an orthogonal coordinate system. Note that solution (10) exactly coincides with the one-dimensional analog of the Kajiura equation (1), which is additional confirmation of the correctness of the displacement potential concept.

A more complex case, for which there is also an analytical solution to problem (2)–(5), is a reservoir with a flat sloping bottom [16, 50]. In this case, it is convenient to use the cylindrical coordinate system (r, φ) (Fig. 1). Problem (2)–(5) in a cylindrical coordinate system is written as follows:

$$r^2\frac{\partial^2 F}{\partial r^2} + r\frac{\partial F}{\partial r} + \frac{\partial^2 F}{\partial \varphi^2} = 0, \tag{11}$$

$$F\big|_{\varphi=0} = 0, \tag{12}$$

$$\frac{1}{r}\frac{\partial F}{\partial \varphi}\bigg|_{\varphi=-\alpha} = d_n(r), \tag{13}$$

$$\xi(r) = \frac{1}{r}\frac{\partial F}{\partial \varphi}\bigg|_{\varphi=0}. \tag{14}$$

We introduce the notations $\chi = \ln(r)$ and $d_\chi(\chi) = rd_n(r)/e^\chi$. In these notations, the solution to problem (11)–(14) has the form

$$\xi(r) = \frac{1}{r\sqrt{2\pi}}\int_{-\infty}^{+\infty} dq\,\frac{1}{\mathrm{ch}(q\alpha)}H(q)e^{iq\chi}, \tag{15}$$

$$\text{where}\quad H(q) = \frac{1}{\sqrt{2\pi}}\int_{-\infty}^{+\infty} d\chi\left(e^\chi d_\chi(\chi)\right)e^{-iq\chi}. \tag{16}$$

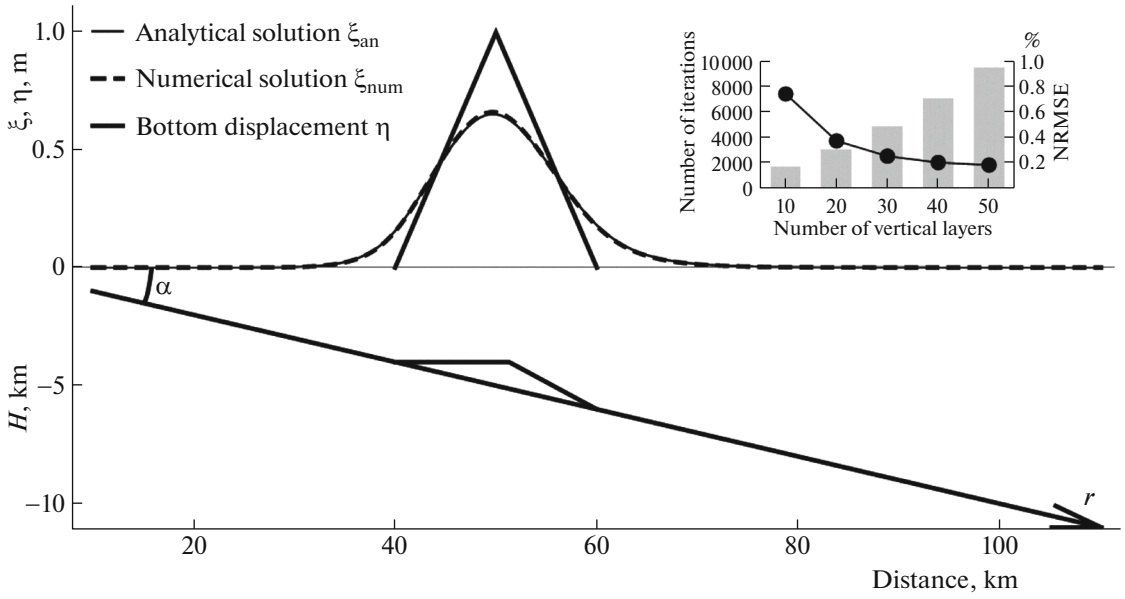

Fig. 1. Statement and solution of the problem of calculating the initial elevation of the water surface, caused by the instantaneous deformation of the bottom of a triangular shape in a basin with a flat sloping bottom. The inset shows the results of comparing the numerical and analytical solutions for different numbers of vertical layers. The normalized standard deviation of one solution from another is shown in black, gray bars show the number of iterations.

The details of the derivation of formulas (15) and (16) are described in detail in ([50], formulas (2.1.1)–(2.1.14)). In general, integrals (15) and (16) are not calculated analytically. However, for some kinds of $d_n(r)$ functions integral (16) is taken analytically and then the calculation of the initial elevation is reduced to taking only integral (15). For example, this can be done if the deformation of the bottom has a rectangular shape $d_n(r) = \eta_0\left(\theta(r - R_1) - \theta(r - R_2)\right)$ [16]. However, this case is also inconvenient for checking the numerical model due to the stepwise form of the $d_n(r)$ function.

Another case in which integral (16) can be taken analytically is the deformation of the bottom of a triangular shape (Fig. 1)

$$d_n(r) = (a_1 r + b_1)\left(\theta(r - R_1) - \theta(r - R_2)\right) + (a_2 r + b_2)\left(\theta(r - R_2) - \theta(r - R_3)\right), \tag{17}$$

where coefficients a_1, a_2, b_1, and b_2 are expressed in terms of the coordinates of the vertices of the triangle. Formula (17) is the sum of two terms of the same form:

$$d_n(r) = (ar + b)\left(\theta(r - R_1) - \theta(r - R_2)\right); \tag{18}$$

therefore, taking integral (16) analytically for the bottom deformation (18) and calculating the corresponding integral (15) numerically, it is possible, using the superposition principle, to obtain the initial elevation caused by the triangular bottom deformation (17).

We substitute the bottom deformation (18) into (16) and then into (15) and obtain

$$\xi(r) = \frac{1}{2\pi r}\int_{-\infty}^{+\infty} dq\Omega(q), \tag{19}$$

where $\Omega(q) = \dfrac{-i}{\mathrm{ch}(q\alpha)}\left(\dfrac{a(R_1^{2-iq} - R_2^{2-iq})}{2i + q} + \dfrac{b(R_1^{1-iq} - R_2^{1-iq})}{i + q}\right)e^{iq\ln(r)}$.

We separate the real and imaginary parts of $\Omega(q)$:

$$\mathrm{Re}\left[\Omega(q)\right] = \frac{1}{\mathrm{ch}(q\alpha)}\frac{b}{1 + q^2}\left(R_2\cos(q\delta_2) - qR_2\sin(q\delta_2) - R_1\cos(q\delta_1) + qR_1\sin(q\delta_1)\right)$$
$$+ \frac{1}{\mathrm{ch}(q\alpha)}\frac{a}{4 + q^2}\left(2R_2^2\cos(q\delta_2) - qR_2^2\sin(q\delta_2) - 2R_1^2\cos(q\delta_1) + qR_1^2\sin(q\delta_1)\right),$$

$$\mathrm{Im}[\Omega(q)] = \frac{1}{\mathrm{ch}(q\alpha)}\frac{b}{1+q^2}\left(R_2\sin(q\delta_2) + qR_2\cos(q\delta_2) - R_1\sin(q\delta_1) - qR_1\cos(q\delta_1)\right)$$
$$+ \frac{1}{\mathrm{ch}(q\alpha)}\frac{a}{4+q^2}\left(2R_2^2\sin(q\delta_2) + qR_2^2\cos(q\delta_2) - 2R_1^2\sin(q\delta_1) - qR_1^2\cos(q\delta_1)\right),$$

where $\delta_1 = \ln(r/R_1)$ and $\delta_2 = \ln(r/R_2)$. The imaginary part $\Omega(q)$ is an odd function and the real part is even; thus, formula (19) can be simplified to

$$\xi(r) = \frac{1}{\pi r}\int_0^{+\infty} dq\,\mathrm{Re}[\Omega(q)]. \tag{20}$$

Formula (20) makes it possible to calculate the initial elevation of the water surface caused by the instantaneous deformation of the bottom of form (18). When coefficient a in (18) vanishes, the deformation of the bottom takes the form of a rectangle, and the obtained solution coincides with the solution published in [16]. Note that, if necessary, we can set the normal deformation of the bottom, limited by an arbitrary broken line, by taking any number of terms of form (18) required for this. The initial elevation of the water surface caused by such a bottom deformation can be easily calculated using the superposition principle and formula (20).

4. NUMERICAL MODEL TESTING

Solution (20) (Fig. 1) was used to test the numerical model. The computational domain was 100 km long, the bottom slope was 0.1 ($\tan\alpha = 0.1$), and the ocean depth in the computational domain varied from 1 km to 11 km. The normal deformation of the bottom had the shape of an isosceles triangle with a base of 20 km and a height of 1 m (shown schematically in Fig. 1 by the bold solid line). The corresponding vertical displacement of the bottom in Fig. 1 is transferred to the water surface and is shown on the same scale with the initial elevation also by a bold solid line. The grid step along axis 0x was 500 m, which corresponds to the characteristic step of the digital bathymetric data (for example, 15 arcsec in https://www.gebco.net/). The number of layers along the vertical (NZ) ranged from 10 to 50. Each calculation recorded the number of iterations NI and the two-dimensional volume of the initial elevation of the water surface $V = \int_0^{+\infty}\xi(r)dr$; and a pointwise comparison of the numerical solution ξ_{num} and analytical solution ξ_{an} was carried out by computing the normalized standard deviation of one solution from the other:

$$\mathrm{NRMSE} = \frac{1}{\mathrm{Max}[\xi_{\mathrm{an}}(r_n)]}\sqrt{\frac{\sum_{n=1}^{n=NX}\left(\xi_{\mathrm{num}}(r_n) - \xi_{\mathrm{an}}(r_n)\right)^2}{NX}}\times 100\%. \tag{21}$$

The values of NI, V_{num}, V_{an}, and NRMSE recorded for each calculation are presented in Table 1.

Figure 1 shows the results of the calculations for NZ = 20. The numerical solution of the problem is shown by the thick dashed line and the analytical solution is shown by the thin solid line. It can be seen

Table 1. Comparison of numerical and analytical solutions

Number of partitions along vertical NZ	10	20	30	40	50
Number of iterations at numerical calculation of NI	1682	3056	4865	7016	9445
Two-dimensional volume of initial elevation for numerical solution V_{num}, m^2	10039.7	10044.5	10045.9	10046.3	10046.3
Two-dimensional volume of initial elevation for analytical solution V_{an}, m^2	10049.8	10049.8	10049.8	10049.8	10049.8
Relative difference in volumes, $\varepsilon = [(V_{\mathrm{an}} - V_{\mathrm{num}})/V_{\mathrm{an}}] \times 100\%$	0.10	0.05	0.04	0.03	0.03
NRMSE, %	0.74	0.37	0.25	0.20	0.18

that the numerical and analytical solutions coincide almost perfectly. The results of a quantitative comparison of calculations for different values of NZ are graphically displayed in the inset in Fig. 1. As expected, with an increase in the number of vertical layers, the difference between the numerical and analytical solutions decreases, but at the same time, the number of iterations also increases. The two-dimensional volumes of the initial elevations also converge as the number of layers increases (Table 1). Note that the values of the two-dimensional volumes are close to the volume of the bottom deformation V_b = 10049.9 m^2. This is independent confirmation of the correctness of the obtained numerical and analytical solutions.

5. CALCULATION OF THE INITIAL ELEVATIONS FOR REAL EVENTS AND VERIFICATION OF THE KAJIURA FILTER

Having tested the constructed numerical model using an analytical solution for the particular case of a basin with a flat sloping bottom, we used the constructed numerical model to calculate the initial elevation in a basin with an arbitrary bottom topography. We emphasize that it is in this case (a basin with an arbitrary bottom topography) that the use of the σ coordinate becomes especially useful.

We calculated the initial elevations of the water surface during two real events: the Kuril earthquake on January 13, 2007 and the Great East Japan Tohoku earthquake on March 11, 2011. In both cases, the calculations were carried out along a certain section directed perpendicular to the deep-water trench (Figs. 2a, 3a). The digital atlas GEBCO2014 was used as the source of the bathymetric data. The bottom deformations were calculated by Okada's formulas [51] using the code ffaultdisp (http://ocean.phys.msu.ru/projects/ffaultdisp/). The ffaultdisp input consists of .fsp files that are freely available on the USGS website (https://earthquake.usgs.gov/). The .fsp files were updated on the USGS website on October 17, 2018. The horizontal bottom deformation component, obtained as a result of using the ffaultdisp, was projected onto the direction of the section and substituted into the numerical model together with the vertical component. The horizontal step in the numerical calculations was 500 m, there were NZ = 20 vertical partitions (see Table 1). The results of the numerical calculations are shown in Figs. 2b and 3b with a thick dashed line.

Note that the concept of the displacement potential, which is the base of our numerical model, is the optimal approach to setting the initial conditions for the problem of the propagation of a tsunami in the instantaneous tsunami generation approximation. The theoretical substantiation of this statement is presented in [15]. Therefore, the numerical solution we obtained can be used as a benchmark for testing

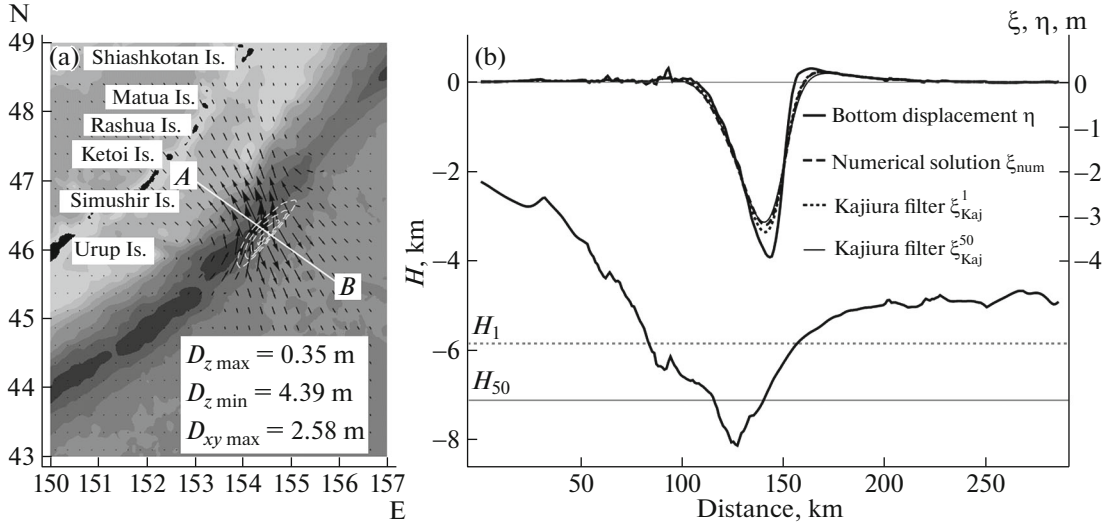

Fig. 2. (a) Bottom deformation area during the Kuril earthquake on January 13, 2007. White dashed isolines are bottom subsidence, isoline spacing is 1 m, arrows are horizontal displacements of the bottom. Segment *AB* shows the section along which two-dimensional calculations were carried out. (b) Bottom profile (thick solid line), vertical displacement of the bottom transferred to the water surface (thick solid line) and initial elevations along section *AB*, calculated by different methods. Horizontal straight lines show average depths by source H_1 (dotted line) and H_{50} (thin solid line) used in the Kajiura filter.

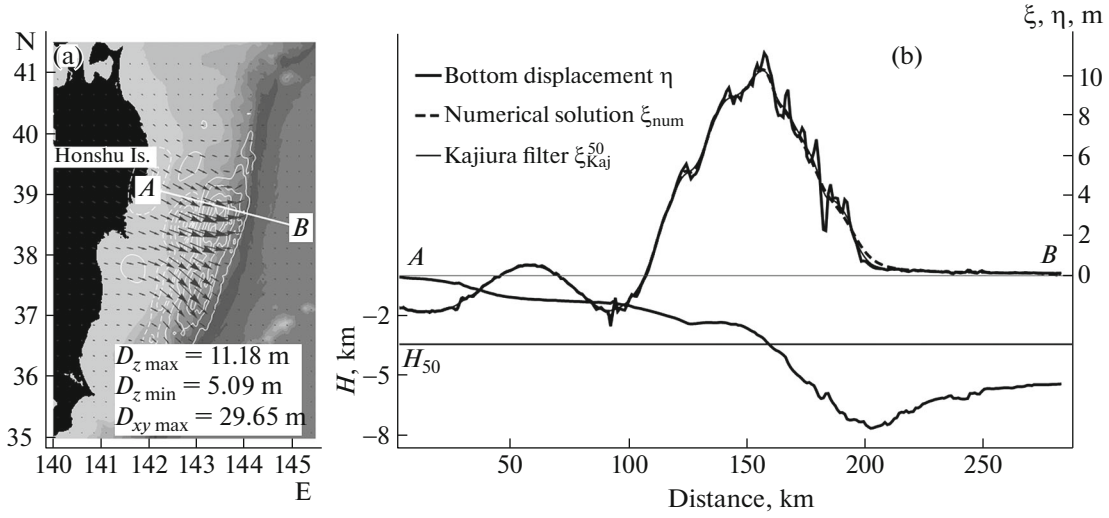

Fig. 3. (a) Bottom deformation area during the Great East Japan Tohoku Earthquake on March 11, 2011. White solid isolines are bottom uplift, white dashed lines are subsidence, isoline spacing is 1 m, arrows are horizontal displacements of the bottom. Segment *AB* shows the section along which two-dimensional calculations were carried out. (b) Bottom profile (thick solid line), vertical displacement of the bottom transferred to the water surface (thick solid line), and initial elevations along section *AB*, calculated by different methods. The horizontal thin straight line shows the average depth at the source H_{50} used in the Kajiura filter.

approximate methods for finding the initial elevation. The results of testing one of these approximate methods (the Kajiura filter) are also given below.

5.1. Kuril Earthquake on January 13, 2007

It can be seen from Fig. 2b that, for the Kuril earthquake, the amplitude of the initial elevation is noticeably smaller than the amplitude of the vertical displacement of the bottom (by 0.71 m or 18%). The smoothing effect in this event manifests itself so clearly for two reasons: firstly, the region of the maximum bottom displacements is located at the bottom of the deep-water trench (from 6 to 8 km, Fig. 2b), and secondly, it has a relatively small horizontal extent (about 35 km) [15, 33, 38]. It is also worth noting that the maximum of the smoothed initial elevation of the water surface is slightly shifted relative to the maximum vertical displacement of the bottom (by 3.5 km). The reason for this is that those areas of bottom displacement that lie at a greater depth are smoothed more strongly and those that lie at a shallower depth are smoothed more weakly.

We use the obtained results to check the approximate method for calculating the initial elevation: the Kajiura filter. In order to apply the Kajiura filter, it is first necessary to calculate the average depth according to the tsunami source. Taking into account that the bathymetry data are known only in a discrete set of points, we proceed as follows. We calculate the vertical displacement of the bottom η [9, 10]

$$\eta = d_z + \frac{dH}{dx} d_x \tag{22}$$

and find the maximum modulo value of η throughout the deformation region. Next, we select the points at which modulo η is more than 1% of this maximum value, and using the bathymetry data, we calculate the average depth H_1 for these points. Then we select the points where η is more than 50% of the maximum value, and calculate H_{50} for them. The obtained values (H_1 = 5845 m and H_{50} = 7118 m) and the vertical displacement of bottom (22) are substituted into the Kajiura equation (10). The results of the calculation of the initial elevation obtained in this way are shown in Fig. 2b by the dotted (for H_1) and thin solid (for H_{50}) lines.

The following integral characteristics were calculated for a quantitative comparison of the initial elevations obtained from the numerical solution of the static problem and using the Kajiura filter: two-dimensional volume $V = \int_0^{+\infty} \xi(r)dr$ and potential energy $E = 0.5\rho g \int_0^{+\infty} \xi^2(r)dr$ (ρ = 1030 kg/m^3 and

Table 2. Comparison of the integral characteristics of the initial elevations calculated by different methods for the Kuril earthquake on January 13, 2007 and the Great East Japan Tohoku earthquake on March 11, 2011

	Jan 13, 2007	Mar 11, 2011
$\lvert V_\eta \rvert$, m^2	78749	483983
$\lvert V_{num} \rvert$, m^2	78483 (−0.3% $\lvert V_\eta \rvert$)	482896 (−0.2% $\lvert V_\eta \rvert$)
$\lvert V^1_{Kaj} \rvert$, m^2	78746 (−0.004% $\lvert V_\eta \rvert$)	
$\lvert V^{50}_{Kaj} \rvert$, m^2	78748 (−0.001% $\lvert V_\eta \rvert$)	485876 (+0.4% $\lvert V_\eta \rvert$)
E_η, $\times 10^9$ J/m	1.29	21.69
E_{num}, $\times 10^9$ J/m	1.03 (−20% E_η)	21.11 (−2.7% E_η)
E^1_{Kaj}, $\times 10^9$ J/m	1.08 (−16% E_η)	
E^{50}_{Kaj}, $\times 10^9$ J/m	1.00 (−22% E_η)	21.21 (−2.2% E_η)

$g = 9.81$ m/s^2). The calculations were carried out for the vertical displacement of bottom η, for the initial elevation found from the complete solution of the static problem ξ_{num}, and for the initial elevations found using the Kajiura filter ξ^1_{Kaj} and ξ^{50}_{Kaj}. The calculation results are summarized in Table 2.

The Kajiura filter overestimates (in absolute value) the amplitude of the initial elevation of the water surface compared to the numerical solution of the static problem by 0.14 m (4%) when used as the average depth H_1 and understates the same amplitude by 0.02 m (0.8%) when used as the average depth H_{50}. From this, a useful practical recommendation follows for researchers using the Kajiura filter: when choosing the average depth by the source, it is necessary to consider only the region of the maximum bottom deformations and substitute it in formula (10) as the average depth, for example, H_{50}. Table 2 shows that the two-dimensional volumes are close to each other in all cases (the difference does not exceed 0.5%). The volume calculated for solving the static problem is the smallest, due to the relatively small number of vertical partitions (see also Table 1). The potential energy of the smoothed initial elevation is 20% less than the potential energy of the bottom vertical displacement. This agrees with the above estimates for the amplitudes of the initial elevation and is explained in a similar way. The same point can be made about the potential energies calculated using the Kajiura filter.

5.2. The Great East Japan Tohoku Earthquake on March 11, 2011

Let us now consider in more detail the results obtained for the earthquake in Japan on March 11, 2011. It can be seen from Fig. 3b that in this case the smoothing effect is mainly manifested not in the decrease in the amplitude of the initial elevation but in the spatial filtering of the vertical displacement of the bottom. Mathematically, this is explained as follows. According to formula (10), the spatial spectrum of the initial elevation of the water surface is modulated by the rapidly decaying function $1/\mathrm{ch}(kH_0)$, where k is the wave number. Consequently, the bottom movements cannot create disturbances on the surface with the wavelength $\lambda < H_0$. Figure 3b clearly shows that the short-wavelength components of the bottom's vertical displacement are indeed not transferred to the surface due to the smoothing effect being taken into account. Note that in the numerical simulation of the tsunami propagation, to adequately reproduce these nonexistent components, it would be necessary to reduce the steps in space and time, which would lead to an increase in the computation time. Thus, taking into account the smoothing effect not only makes it possible to avoid errors in the calculation of the amplitude of the initial elevation but also improves the efficiency of the numerical models [16, 17, 52].

The average depths that needed to be applied to the Kajiura filter in this case were $H_1 = 3456$ m and $H_{50} = 3438$ m. Considering that the obtained values are close to each other, as well as the conclusions obtained in the analysis of the Kuril event, in this case, we carried out calculations using the Kajiura formula only for H_{50}. A noticeable difference between the numerical solution of the static problem and the calculations using the Kajiura formula is observed only in shallow water. There, the Kajiura filter smooths out the short-wavelength components of the bottom displacement much more strongly than the solution

of the static problem. This is logical, since the depth H_{50}, used in the Kajiura filter, is obviously greater than the depth of the ocean in shallow water. The results of a quantitative comparison of the two approaches to the calculation of the initial elevation are shown in Table 2. It can be seen that the volumes in this case also differ by less than 0.5%, and in terms of the potential energy, the role of the smoothing effect can be estimated at 2–3% (for both methods of calculating the initial elevation).

6. RESULTS AND DISCUSSION

A two-dimensional ($0xz$) numerical model that makes it possible to calculate the initial elevation of the water surface in the source of a tsunami in a basin of variable depth is constructed. The model is developed in the approximation of an instantaneous deformation of the bottom and allows us to set the deformation of the bottom of an arbitrary shape. The model takes into account the smoothing effect of the water layer and the contribution of the horizontal components of the bottom deformation. The construction and testing of such a model is a necessary methodological step in preparing for the numerical solution of the complete three-dimensional problem of calculating the initial elevation in a basin with an arbitrary bottom topography. In particular, the two-dimensional model makes it possible to work out the use of nonorthogonal coordinates $(\hat{x}, \sigma)$ and adapt the iteration method for the given task.

To test the numerical model, an analytical solution was obtained for the problem of calculating the initial elevation for the case of a normal deformation of a flat, inclined bottom, which has a triangular shape. This solution is valuable not only for testing this two-dimensional model but also for testing a future three-dimensional model, if such testing is carried out on an extended earthquake source along the $0y$ axis. Moreover, it is highly likely that this solution will be the only possible test for a 3D model, as obtaining a three-dimensional analytical solution of the static problem of the initial elevation in a basin with a flat sloping bottom is associated with significant mathematical difficulties (Bessel functions of an imaginary order, etc.).

The initial elevations of the water surface along arbitrarily chosen sections for the Kuril earthquake on January 13, 2007 and the Great East Japan Tohoku earthquake on March 11, 2011 are calculated using the constructed two-dimensional numerical model. The numerically calculated initial elevations are used to test an approximate method for calculating the initial elevation: the Kajiura filter. By comparison with the numerical solution, it was found that it is advisable to take the average depth of the region of the maximum bottom deformations as the average depth of the tsunami source. A method for calculating such an average depth is given.

ACKNOWLEDGMENTS

The authors thank the reviewer for his numerous valuable comments that contributed to a significant improvement of the manuscript.

FUNDING

This study was supported by the Russian Science Foundation, grant no. 22-27-00415; https://rscf.ru/project/22-27-00415/.

CONFLICT OF INTEREST

The authors declare that they have no conflicts of interest.

REFERENCES

1. M. A. Nosov, "Tsunami waves of seismic origin: The modern state of knowledge," Izv. Atmos. Ocean. Phys. **50** (5), 474–484 (2014). https://doi.org/10.1134/S0001433814030098
2. A. R. Gusman, I. E. Mulia, K. Satake, S. Watada, M. Heidarzadeh, and A. F. Sheehan, "Estimate of tsunami source using optimized unit sources and including dispersion effects during tsunami propagation: The 2012 Haida Gwaii earthquake," Geophys. Res. Lett. **43** (18), 9819–9828 (2016). https://doi.org/10.1002/2016GL070140
3. G. C. Lotto, G. Nava, and E. M. Dunham, "Should tsunami simulations include a nonzero initial horizontal velocity?," Earth, Planets Space **69** (1), 117, 1–14 (2017). https://doi.org/10.1186/s40623-017-0701-8

4. T. Maeda and T. Furumura, "FDM simulation of seismic waves, ocean acoustic waves, and tsunamis based on tsunami-coupled equations of motion," Pure Appl. Geophys. **170** (1), 109–127 (2013). https://doi.org/10.1007/s00024-011-0430-z
5. J. E. Kozdon and E. M. Dunham, "Constraining shallow slip and tsunami excitation in megathrust ruptures using seismic and ocean acoustic waves recorded on ocean-bottom sensor networks," Earth Planet. Sci. Lett. **396**, 56–65 (2014). https://doi.org/10.1016/j.epsl.2014.04.001
6. G. C. Lotto, T. N. Jeppson, and E. M. Dunham, "Fully coupled simulations of megathrust earthquakes and tsunamis in the Japan Trench, Nankai Trough, and Cascadia Subduction Zone," Pure Appl. Geophys. **176**, 4009–4041 (2019). https://doi.org/10.1007/s00024-018-1990-y
7. S. Popinet, "Adaptive modelling of long-distance wave propagation and fine-scale flooding during the Tohoku tsunami," Nat. Hazards Earth Syst. Sci. **12** (4), 1213–1227 (2012). https://doi.org/10.5194/nhess-12-1213-2012
8. S. Iwasaki, "Experimental study of a tsunami generated by a horizontal motion of a sloping bottom," Bull. Earthquake Res. Inst. **57**, 239–262 (1982).
9. Y. Tanioka and K. Satake, "Tsunami generation by horizontal displacement of ocean bottom," Geophys. Res. Lett. **23** (8), 861–864 (1996). https://doi.org/10.1029/96GL00736
10. M. A. Nosov, A. V. Bolshakova, and S. V. Kolesov, "Displaced water volume, potential energy of initial elevation, and tsunami intensity: Analysis of recent tsunami events," Pure Appl. Geophys. **171** (12). 3515–3525 (2014). https://doi.org/10.1007/s00024-013-0730-6
11. A. V. Bolshakova, M. A. Nosov, and S. V. Kolesov, "The properties of co-seismic deformations of the ocean bottom as indicated by the slip-distribution data in tsunamigenic earthquake sources," Moscow Univ. Phys. Bull. **70** (1), 62–67 (2015). https://doi.org/10.3103/S0027134915010038
12. M. A. Nosov, A. V. Bolshakova, and K. A. Sementsov, "Energy characteristics of tsunami sources and the mechanism of wave generation by seismic movements of the ocean floor," Moscow Univ. Phys. Bull. **76**, S136–S142 (2021). https://doi.org/10.3103/S0027134922010076
13. R. Takahashi, "On seismic sea waves caused by deformations of the sea bottom," Bull. Earthquake Res. Inst. **20**, 357–400 (1942).
14. K. Kajiura, "The leading wave of a tsunami," Bull. Earthquake Res. Inst. **41**, 535–571 (1963).
15. M. A. Nosov and S. V. Kolesov, "Optimal initial conditions for simulation of seismotectonic tsunamis," Pure Appl. Geophys. **168** (6–7), 1223–1237 (2011). https://doi.org/10.1007/s00024-010-0226-6
16. M. A. Nosov and K. A. Sementsov, "Calculation of the initial elevation at the tsunami source using analytical solutions," Izv. Atmos. Ocean. Phys. **50** (5), 539–546 (2014). https://doi.org/10.1134/S0001433814050089
17. M. A. Nosov, *Introduction to Tsunami Wave Theory* (Yanus-K, Moscow, 2019) [in Russian].
18. K. Aki and P. G. Richards, *Quantitative Seismology*, 2nd ed. (Univ. Sci. Books, Sausalito, CA, 2002).
19. C. Ji, D. J. Wald, and D. V. Helmberger, "Source description of the 1999 Hector Mine, California, earthquake, Part I: Wavelet domain inversion theory and resolution analysis," Bull. Seismol. Soc. Am. **92** (4), 1192–1207 (2002). https://doi.org/10.1785/0120000916
20. S. E. Minson, J. R. Murray, J. O. Langbein, and J. S. Gomberg, "Real-time inversions for finite fault slip models and rupture geometry based on high-rate GPS data," J. Geophys. Res.: Solid Earth **119**, 3201–3231 (2014). https://doi.org/10.1002/2013JB010622
21. S. Kawamoto, Y. Ohta, Y. Hiyama, M. Todoriki, T. Nishimura, T. Furuya, Y. Sato, T. Yahagi, and K. Miyagawa, "REGARD: A new GNSS-based real-time finite fault modeling system for GEONET," J. Geophys. Res.: Solid Earth **122**, 1324–1349 (2017).
22. S. Watada, S. Kusumoto, and K. Satake, "Traveltime delay and initial phase reversal of distant tsunamis coupled with the self-gravitating elastic Earth," J. Geophys. Res.: Solid Earth **119**, 4287–4310 (2014).
23. T.-C. Ho, K. Satake, and S. Watada, "Improved phase corrections for transoceanic tsunami data in spatial and temporal source estimation: Application to the 2011 Tohoku earthquake," J. Geophys. Res.: Solid Earth **122** (12), 10155–10175 (2017). https://doi.org/10.1002/2017JB015070
24. J. L. Hammack, "A note on tsunamis: their generation and propagation in an ocean of uniform depth," J. Fluid Mech. **60** (4), 769–799 (1973). https://doi.org/10.1017/S0022112073000479

25. S. N. Ward, "Tsunamis," in *The Encyclopedia of Physical Science and Technology*, 3rd ed., Ed. by R. A. Meyers (Academic Press, San Diego, 2001), Vol. 17, pp. 175–191.
26. Y. Kervella, D. Dutykh, and F. Dias, "Comparison between three-dimensional linear and nonlinear tsunami generation models," Theor. Comput. Fluid Dyn. **21** (4), 245–269 (2007). https://doi.org/10.1007/s00162-007-0047-0
27. T. Saito and T. Furumura, "Three-dimensional tsunami generation simulation due to sea-bottom deformation and its interpretation based on the linear theory," Geophys. J. Int. **178** (2), 877–888 (2009). https://doi.org/10.1111/j.1365-246X.2009.04206.x
28. Y. Tanioka and T. Seno, "Sediment effect on tsunami generation of the 1896 Sanriku tsunami earthquake," Geophys. Res. Lett. **28** (17), 3389–3392 (2001). https://doi.org/10.1029/2001GL013149
29. H. Tsushima, R. Hino, Y. Tanioka, F. Imamura, and H. Fujimoto, "Tsunami waveform inversion incorporating permanent seafloor deformation and its application to tsunami forecasting," J. Geophys. Res. **117**, B03311 (2012). https://doi.org/10.1029/2011JB008877
30. T. Baba, Y. Gon, K. Imai, K. Yamashita, T. Matsuno, M. Hayashi, and H. Ichihara, "Modeling of a dispersive tsunami caused by a submarine landslide based on detailed bathymetry of the continental slope in the Nankai trough, southwest Japan," Tectonophys. **768**, 228182 (2019). https://doi.org/10.1016/j.tecto.2019.228182
31. T. Saito, "Tsunami generation: validity and limitations of conventional theories," Geophys. J. Int. **210** (3), 1888–1900 (2017). https://doi.org/10.1093/gji/ggx275
32. T. Baba, S. Allgeyer, J. Hossen, P. R. Cummins, H. Tsushima, K. Imai, K. Yamashita, and T. Kato, "Accurate numerical simulation of the far-field tsunami caused by the 2011 Tohoku earthquake, including the effects of Boussinesq dispersion, seawater density stratification, elastic loading, and gravitational potential change," Ocean Modell. **111**, 46–54 (2017). https://doi.org/10.1016/j.ocemod.2017.01.002
33. I. V. Fine and E. A. Kulikov, "Calculation of sea surface displacements in a tsunami source area caused by instantaneous vertical deformation of the seabed due to an underwater earthquake," Vychisl. Tekhnol. **16** (2), 111–118 (2011).
34. T. Saito, "Dynamic tsunami generation due to sea-bottom deformation: Analytical representation based on linear potential theory," Earth, Planets Space **65** (12), 1411–1423 (2013). https://doi.org/10.5047/eps.2013.07.004
35. E. A. Kulikov, V. K. Gusiakov, A. A. Ivanova, and B. V. Baranov, "Numerical tsunami modelling and the bottom relief," Moscow Univ. Phys. Bull. **71** (6), 527–536 (2016). https://doi.org/10.3103/S002713491605012X
36. E. A. Kulikov, A. Yu. Medvedeva, and I. V. Fain, "Tsunami hazard assessment in the Caspian Sea," Okeanol. Issled. (Oceanol. Res.) **47** (5), 74–88 (2019). https://doi.org/10.29006/1564-2291.JOR-2019.47(5).6
37. T. Saito, *Tsunami Generation and Propagation* (Springer, Tokyo, 2019). https://doi.org/10.1007/978-4-431-56850-6
38. M. A. Nosov and S. V. Kolesov, "Method of specification of the initial conditions for numerical tsunami modeling," Moscow Univ. Phys. Bull. **64** (2), 208–213 (2009). https://doi.org/10.3103/S0027134909020222
39. O. M. Phillips, "On the generation of waves by turbulent wind," J. Fluid Mech. **2** (5), 417–445 (1957). https://doi.org/10.1017/S0022112057000233
40. Y.-Y. Li, B. Wang, and D.-H. Wang, "Characteristics of a terrain-following sigma coordinate," Atmos. Ocean. Sci. Lett. **4** (3), 157–161 (2011). https://doi.org/10.1080/16742834.2011.11446922
41. S. M. Griffies, C. Böning et al., "Developments in ocean climate modelling," Ocean Modell. **2** (3-4), 123–192 (2000). https://doi.org/10.1016/S1463-5003(00)00014-7
42. A. V. Gusev, "Numerical model of ocean hydrodynamics in curvilinear coordinates for reproducing the circulation of the world ocean and its separate water areas," Candidate's Dissertation in Physics and Mathematics (Inst. Vychisl. Mat., Moscow, 2009).
43. N. A. Dianskii, *Modeling Ocean Circulation and Studying Its Response to Short-Term and Long-Term Atmospheric Impacts* (Fizmatlit, Moscow, 2013) [in Russian].
44. M. A. Nosov and S. V. Kolesov, "Combined numerical model of a tsunami," Math. Models Comput. Simul. **11** (5), 679–689 (2019). https://doi.org/10.1134/S2070048219050156

45. K. A. Sementsov, M. A. Nosov, S. V. Kolesov, V. A. Karpov, H. Matsumoto, and Y. Kaneda, "Free gravity waves in the ocean excited by seismic surface waves: Observations and numerical simulations," J. Geophys. Res. Oceans **124** (11), 8468–8484 (2019). https://doi.org/10.1029/2019JC015115
46. R. L. Haney, "On the pressure gradient force over steep topography in sigma coordinate ocean models," J. Phys. Oceanogr. **21** (4), 610–619 (1991). https://doi.org/10.1175/1520-0485(1991)021<0610:OTPGFO>2.0.CO;2
47. A. Beckmann and D. B. Haidvogel, "Numerical simulation of flow around a tall isolated seamount. Part I: Problem formulation and model accuracy," J. Phys. Oceanogr. **23** (8), 1736–1753 (1993). https://doi.org/10.1175/1520-0485(1993)023<1736:NSOFAA>2.0.CO;2
48. K. A. Sementsov and A. V. Bolshakova, "A model for the generation of waves in the ocean by seismic bottom movements in sigma-coordinates," Moscow Univ. Phys. Bull. **75** (1), 87–94 (2020). https://doi.org/10.3103/S0027134920010129
49. A. A. Samarskii, *Introduction to the Theory of Difference Schemes* (Nauka, Moscow, 1971) [in Russian].
50. K. A. Sementsov, "Dynamic and static models of generation of surface gravity waves in the ocean by earthquakes," Candidate's Dissertation in Physics and Mathematics (Mosk. Gos. Univ. im. M. V. Lomonosova, Moscow, 2017).
51. Y. Okada, "Surface deformation due to shear and tensile faults in a half-space," Bull. Seismol. Soc. Am. **75** (4), 1135–1154 (1985). https://doi.org/10.1785/BSSA0750041135
52. B. W. Levin and M. A. Nosov, *Physics of Tsunamis*, 2nd ed. (Springer, Cham, 2016). https://doi.org/10.1007/978-3-319-24037-4